JOURNAL OF AGRICULTURAL AND FOOD CHEMISTRY

pubs.acs.org/JAFC Article

Expanding the Chemical Space of Succinate Dehydrogenase Inhibitors via the Carbon−Silicon Switch Strategy

Ge Wei,[§] Ming-Wei Huang,[§] Wen-Jie Wang, Yuan Wu, Shu-Fen Mei, Li-Ming Zhou, Long-Can Mei, Xiao-Lei Zhu,* and Guang-Fu Yang*

Cite This: *J. Agric. Food Chem.* 2021, 69, 3965−3971 Read Online

ACCESS | Metrics & More | Article Recommendations | Supporting Information

ABSTRACT: The carbon−silicon switch strategy has become a key technique for structural optimization of drugs to widen the chemical space, increase drug activity against targeted proteins, and generate novel and patentable lead compounds. Flubeneteram, targeting succinate dehydrogenase (SDH), is a promising fungicide candidate recently developed in China. We describe the synthesis of novel SDH inhibitors with enhanced fungicidal activity to enlarge the chemical space of flubeneteram by employing the C−Si switch strategy. Several of the thus formed flubeneteram-silyl derivatives exhibited improved fungicidal activity against porcine SDH compared with the lead compound flubeneteram and the positive controls. Disease control experiments conducted in a greenhouse showed that trimethyl-silyl-substituted compound **W2** showed comparable and even higher fungicidal activities compared to benzovindiflupyr and flubeneteram, respectively, even with a low concentration of 0.19 mg/L for soybean rust control. Furthermore, compound **W2** encouragingly performed slightly better control than azoxystrobin and was less active than benzovindiflupyr at the concentration of 100 mg/L against soybean rust in field trials. The computational results showed that the silyl-substituted phenyl moiety in **W2** could form strong van der Waals (VDW) interactions with SDH. Our results indicate that the C−Si switch strategy is an effective method for the development of novel SDH inhibitors.

KEYWORDS: *succinate dehydrogenase inhibitors, silicon, soybean rust, docking*

INTRODUCTION

The incorporation of Si into a drug scaffold and substituting C at a specific position of the molecular skeleton (known as the C−Si switch strategy) has become a key approach for widening the chemical space and optimizing the activity of a compound against target proteins, which has led to the recent development and patenting of a novel lead compound.[1−9] Compared to their all carbon counterparts, organosilicon molecules may have significantly improved pharmacological properties, such as improved bioactivity, stability, and pharmacokinetic properties.[10−13] A good example in this regard is silyl-substituted indomethacin derivatives, which exhibit enhanced anticancer activity against a human pancreatic cancer cell line and several human multiple myeloma cell lines compared to the parent indomethacin.[14] In addition, the C−Si switch strategy has also been successfully applied in the preparation of the fungicide flusilazole,[15] silthiofam,[16] and insecticide silafluofen.[17] Maienfisch et al. recently reported improved pharmacological properties in the acaracide sila-cyflumetofen compared to those in cyflumetofen.[18]

Flubeneteram is a promising fungicide candidate recently discovered in China in 2017, containing a pyrazole-carboxamide diphenyl ether moiety, with an IC_{50} value of 0.19 μM against porcine succinate dehydrogenase (SDH).[17] Experiments for determining its biological efficacy showed that flubeneteram displayed excellent protection against *Rhizoctonia solani* and *Sphaerotheca fuliginea*, even at dosages as low as 6.25 mg/L.[17−19] Structure−activity relationships of flubeneteram determined that the inclusion of a diphenyl ether linked to a pyrazole-carboxamide moiety was particularly important for the fungicidal activity of this novel class of SDH inhibitors (SDHIs). Recently, we also found that when the diphenyl ether was connected to the pyrazine-carboxamide, compounds exhibited a 100% inhibitory rate against *Botryotinia fuckeliana* in vitro at a concentration of 20 mg/L and a 95% inhibitory rate against soybean gray mold in vivo at a concentration of 100 mg/L dosage.[20] Indeed, the usefulness of diphenyl ether substituted compounds is increasingly being recognized, and recently we have reviewed the medicinal and agrochemical versatility of the diphenyl ether fragment.[21]

Herein, novel SDHIs have been developed by employing the C−Si switch strategy to widen the chemical space of flubeneteram and thereby increase its fungicidal activity (Figure 1). We report the design, synthesis, and fungicidal activity of a series of flubeneteram-silyl compounds with enhanced fungicidal activity against porcine SDH compared with the lead compound flubeneteram and positive control. Furthermore, the target compounds were investigated for their ability to control several important crop diseases in greenhouse experiments, with most compounds showing particularly high disease control (>80%) against soybean rust (SBR) at a

Received: November 19, 2020
Revised: March 10, 2021
Accepted: March 18, 2021
Published: March 29, 2021

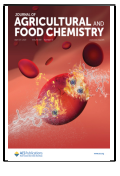

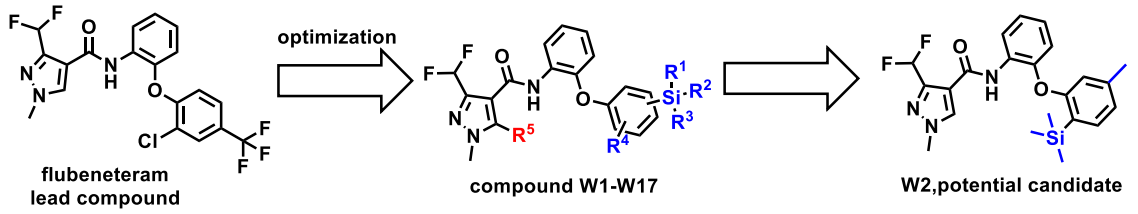

Figure 1. Design protocol of flubeneteram-silyl derivatives.

Scheme 1. Synthetic Route of Compounds, Reagents, and Conditions[a]

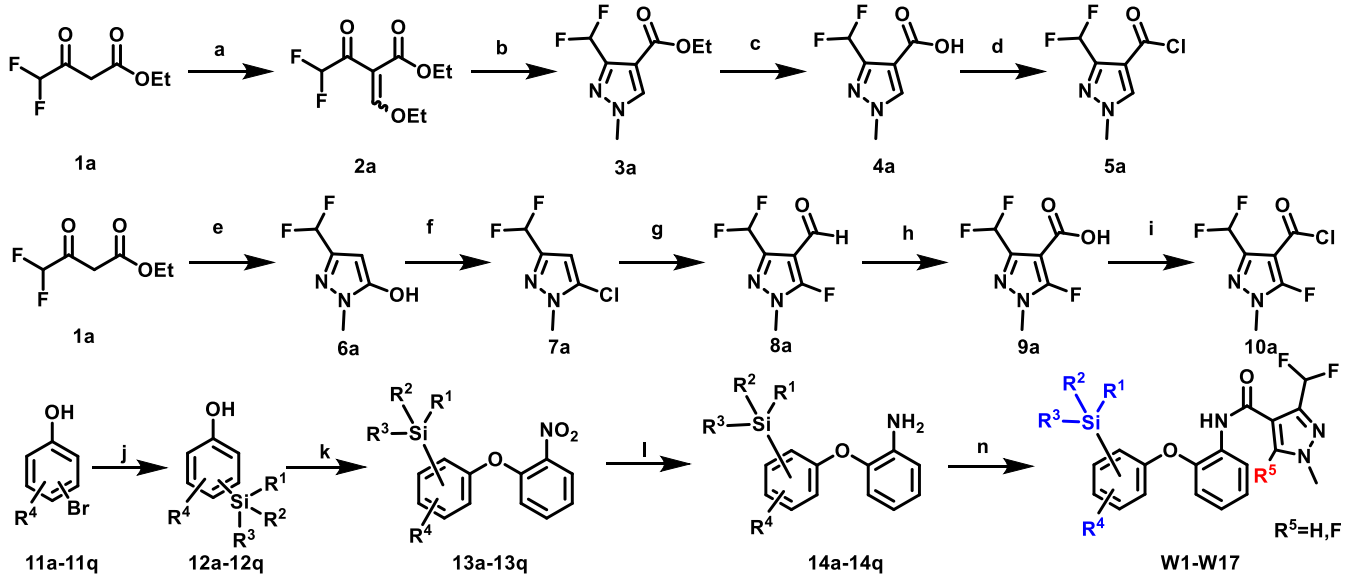

[a](a) triethyl orthoformate, Ac_2O, reflux; (b) methylhydrazine, NaOH, toluene/H_2O; (c) LiOH, THF/H_2O, reflux; (d) $SOCl_2$, reflux; (e) methylhydrazine, toluene, reflux; (f) phosphorus oxychloride, DMF; (g) KF, tetrabutylazanium, DMF; (h) $KMnO_4$, H_2O; (i) $SOCl_2$, reflux; (j) *t*-BuLi, chlorosilane, THF, −78 °C; (k) o-fluoronitrobenzene, K_2CO_3, DMF, reflux; (l) Fe, NH_4Cl, EtOH; and (m) pyrazole-4-carbonyl chloride, Et_3N, CH_2Cl_2.

concentration of 6.25 mg/L. Flubeneteram-silyl analogue **W2** exhibited the most potent fungicidal activity against SBR in both greenhouse and field trials. Further computational simulations revealed that the distal silyl-substituted phenyl moiety in **W1**−**W17** occupied the entrance to the SDH binding site, thereby forming stronger van der Waals (VDW) interactions compared to those in flubeneteram. This further clarifies the structural requirements of SDHIs with high fungicidal activity against SBR.

MATERIALS AND METHODS

Chemistry. Melting points were measured on a BüCHI B-545 melting point apparatus without correction. ^{1}H NMR and ^{13}C NMR spectra were measured on a Varian Mercury-Plus 600 or 400 spectrometer (Varian Inc., Palo Alto, CA) using $CDCl_3$ or DMSO-d_6 as the solvent. High-resolution mass spectra (HRMS) were acquired on a MALDI SYNAPT G2 HDMS (MALDI). Crystal structures were identified on a Bruker Smart Apex charge-coupled device. All reagents and solvents were commercially available and used directly without further purification.

Synthetic Chemistry. Intermediates **5a**, **10a**, and **12a**−**12q** were synthesized according to the previously published methods.[22−24] Detailed synthetic procedures and characterization data for all of the newly synthesized compounds are given in the Supporting Information (SI).

X-ray Diffraction. We used X-ray diffraction to verify the structure of W2 on Bruker Smart Apex DUO. The crystal data and refinement parameters of **W2** are listed in Table 1S (SI), and the crystal structure is shown in Figure 1S (SI). The atomic coordinates of **W2** have been deposited with the Cambridge Crystallographic Data Centre (CCDC-2006730), from where the full crystallographic data can be obtained.

Molecular Docking. The 3D structures of the newly synthesized compounds were constructed based on the crystal structure of **W2** using SYBYL and then minimized with the steepest descent method and conjugate gradient method, both with 2000 steps and a convergence criterion of 0.001 kcal/mol/Å. Molecular docking of the porcine SDH receptor was performed using its crystal structure (PDB ID: 3ABV)[25] and the modeling was performed with Autodock 4.2.[26] In 3ABV, it contains four chains, called A, B, C, and D chains. The binding site was constructed by B, C, and D chains. And then, the A chain was deleted in the following molecular docking. The grid center was set according to the ligand in 3ABV. The grid box was set as 40 × 40 × 40, and the grid space was set at 0.375 Å. The default values were used for other parameters. We acquired 256 possible binding conformations with the conformation search method of the Lamarckian genetic algorithm (LGA),[27] which were then subjected to further energy minimization and short molecular dynamics simulations following our previously established protocol.[28] Finally, the molecular mechanics/Poisson−Boltzmann surface area (MM/PBSA) method was used to calculate the binding energy of the minimized complex structure.[29] The final structure was selected based on the binding energy and binding mode of commercial carboxamide fungicides obtained from our previous study.[30]

Enzymatic Activity. SDH from the porcine heart was prepared following our previously established procedure.[31,32] The enzymatic activities of SDH were analyzed as reported previously.[31,32] The inhibition rates of target compounds were determined at concen-

https://doi.org/10.1021/acs.jafc.0c07322
J. Agric. Food Chem. 2021, 69, 3965−3971

trations of 1 μM, while IC_{50} values were determined by varying inhibitor concentrations. The commercial fungicide pydiflumetofen and benzovindiflupyr were chosen as the positive controls.

Fungicidal Activity in Greenhouse. The protective activities of the target compounds in a greenhouse against soybean rust (SBR: *Phakopsora pachyrhizi* Sydow), wheat powdery mildew (WPM: *Erysiphe graminis*), rice blast (RB: *Pyricularia grisea*), cucumber downy mildew (CDM: *Pseudoperonospora cubensis*), and soybean gray mold (SGM: *Botritis cinerea*) were determined following the pesticide bioassay developed by Shenyang Sinochem Agrochemicals R&D Company Ltd. (Shenyang, China);[33,34] the results are summarized in Tables 3, 2S, and 3S (SI).

Field Trials. Field trials were conducted in the experimental base of Shenyang (Liaoning province) in a plot with an area of 25 m^2, and with soybean plants at the five-leaf stage using the standard method (see SI for full details).

RESULTS AND DISCUSSION

Synthetic Chemistry. A series of novel flubeneteram-silyl derivatives were synthesized, and the general synthetic route is outlined in Scheme 1. The key electrophilic intermediates **5a** and **10a** are the classic pyrazole-4-carbonyl chloride in succinate dehydrogenase inhibitors (SDHIs), and the synthetic routes from our previously published methods were followed.[35] Silyl-substituted phenols **12a−12q** were obtained by the reaction of substituted phenols and chlorosilane in the presence of n-BuLi. The intermediate then reacts with 2-fluoronitrobenzene in DMF and potassium carbonate affording diphenyl ethers **13a−13q**, which were subsequently reduced to generate silyl-substituted 2-aminodiphenyl ethers **14a−14q**. The final coupling step involved the reaction of acyl chlorides **5a** and **10a** with the silyl-substituted amino analogues **14a−14q** to generate the corresponding target compounds **W1−W17** in yields generally exceeding 60%.

The structure of the target compounds was confirmed by ^1H NMR, ^{13}C NMR, and HRMS analyses (see SI). A full crystal structure was obtained for the target compound **W2** (Figure 1S); the crystal data and the structure refinement parameters are shown in Table 1S.

Structure−Activity Relationships. The enzymatic inhibition exhibited by all newly synthesized compounds **W1−W17** against porcine SDH was assayed, and the determined inhibitory rate or IC_{50} values are listed in Table 1. For comparison, the inhibitory activities of commercial fungicides, pydiflumetofen and benzovindiflupyr, as well as the corresponding nonsilyl-containing fungicide candidate flubeneteram, are also presented. Most of the compounds exhibited good inhibitory activity against porcine SDH. Substitution at C-2 of the distal phenyl ring with a trimethyl-silyl moiety in **W4** (IC_{50} = 2.52 μM) led to a higher inhibitory activity than substitution at either C-3 (**W5**, I = 37.49%) or C-4 (**W3**, I = 46.24%). Moreover, even with additional alkyl substitution on the phenyl ring, trimethyl-silyl substitution at C-2 is still found to be optimal for inhibition. For example, **W2** (with R^1−R^3 = Me at C-2 and R^4 = Me at C-5) shows greater inhibition (IC_{50} = 0.23 μM), compared to **W1** (IC_{50} = 1.17 μM) with the same substituents, but switched in position (Table 1). However, when a triethyl-silyl moiety was substituted at C-2, the opposite trend was observed and the inhibitory effect was slightly reduced compared to substitution at C-5 (compare **W7**, IC_{50} = 0.19 μM to **W6**, IC_{50} = 0.13 μM). From these results, we concluded that the compound displayed preferred activity with C-2 silyl-substituted analogues.

Table 1. Inhibition Activities of Compounds W1−W17 against Porcine SDH[a]

No.	Si position	R^1	R^2	R^3	R^4	R^5	I%[a] or IC_{50} (μM)
W1	5	Me	Me	Me	2-Me	H	1.17 ± 0.11
W2	2	Me	Me	Me	5-Me	H	0.23 ± 0.023
W3	4	Me	Me	Me	H	H	46.24%
W4	2	Me	Me	Me	H	H	2.52 ± 0.14
W5	3	Me	Me	Me	H	H	37.49%
W6	5	Et	Et	Et	2-Me	H	0.13 ± 0.0032
W7	2	Et	Et	Et	5-Me	H	0.19 ± 0.016
W8	2	Me	Me	Et	5-Me	H	0.083 ± 0.0062
W9	5	Me	Me	Et	2-Me	H	46.89%
W10	2	Me	Me		5-Me	H	0.086±0.0040
W11	2	Et	Et	Et	H	H	33.03%
W12	2	n-Pr	n-Pr	n-Pr	5-Me	H	0.034 ± 0.0016
W13	2	Me	Me		5-Me	H	0.27 ± 0.022
W14	2	n-Bu	n-Bu	n-Bu	5-Me	H	41.00%
W15	2	Me	Me	Me	5-Me	F	0.25 ± 0.025
W16	2	Me	Me	Et	5-Me	F	0.44 ± 0.040
W17	2	Me	Me	Me	H	F	0.62 ± 0.034
		flubeneteram					0.19 ± 0.017
		pydiflumetofen					0.13 ± 0.01
		benzovindiflupyr					0.091 ± 0.0059

[a]I = inhibition rate tested at 1 μM concentration.

With this in mind, we investigated the effect of varying the steric bulk of the groups R^1−R^3 at C-2 of the distal phenyl group on the compound activity. We found that increasing the steric bulk of R^1−R^3 (R^4 = 5-methyl) increased the activity of the target compounds against porcine SDH, as observed by comparing **W2** (R^1−R^3 = methyl, IC_{50} = 0.23 μM), **W7** (R^1−R^3 = ethyl, IC_{50} = 0.19 μM), and **W12** (R^1−R^3 = *n*-Pr, IC_{50} = 0.034 μM). However, an excessively large alkyl-substituted silyl moiety was deleterious for the activity, and when R^1−R^3 was increased to *n*-butyl as in **W14**, the inhibitory rate decreased to 41% compared with **W2** (IC_{50} = 0.23 μM). In addition, the same steric effect was also observed by single substitution on the silyl moiety, such as in **W8**, which has a greater inhibition (R^1, R^2 = methyl, R^3 = ethyl; IC_{50} = 0.083 μM), than **W2** (R^1−R^3 = methyl). The inhibition with **W8** was comparable to that with **W10** (R^1, R^2 = methyl, R^3 = trifluoropropyl; IC_{50} = 0.086 μM) but, in any case, considerably greater than **W2**, which confirms our finding of greater inhibition as the steric bulk in R^1−R^3 increases. However, the similar inhibitory rate in **W13** (R^1, R^2 = methyl, R^3 = allyl, IC_{50} = 0.27 μM) compared to **W2** despite the increased steric bulk in **W13** suggests that the interaction between SDH and inhibitor is intricate.

Liu et al. reported that fluorine substitution in pyrazole rings enhanced compound activities.[34,36−39] Considering the enhancement in properties brought about by the incorporation of fluorine into the pyrazole ring of SDHIs, compounds **W15−W17** were generated containing a fluorine atom in the pyrazole ring at R^5 (Figure S1). In general, except for **W17**, the fluorine-substituted analogues **W15** (IC_{50} = 0.25 μM) and **W16** (IC_{50} = 0.44 μM) exhibited lower activities than their hydrogen-containing counterparts **W2** (IC_{50} = 0.23 μM) and **W8** (IC_{50} = 0.083 μM), respectively. Overall, these results indicate that the fungicidal activity is influenced by both the nature of the aliphatic substituents on the silyl group and its position within the phenyl group.

Evaluating our results, we can see that the optimal fungicidal activity was obtained with **W12** (IC_{50} = 0.034 μM), which is more active than benzovindiflupyr (IC_{50} = 0.091 μM), pydiflumetofen (IC_{50} = 0.13 μM), and flubeneteram (IC_{50} = 0.19 μM), by about 3, 4, and 6 times, respectively.

https://doi.org/10.1021/acs.jafc.0c07322
J. Agric. Food Chem. 2021, 69, 3965−3971

Binding Free Energy Calculation. To further understand the structure−activity relationships (SARs) at the atomic level, we performed molecular docking and binding energy calculations for target compounds with determined IC_{50} values. As summarized in Table 2, the calculated binding energies (ΔG_{cal}) ranged from −30.38 to −36.28 kcal/mol, whereas the experimental binding energies (ΔG_{exp} = $-RTLnIC_{50}$) ranged from −7.66 to −10.21 kcal/mol. While it is evident that the MM-PBSA calculations systematically overestimated the absolute binding affinities of the ligand toward SDH, the same trend in binding energies for the target compounds (ΔG_{cal}) was observed as in the experimental energies (ΔG_{exp}), with the correlation coefficient R^2 0.93 between them (Figure 2S, SI), indicating the reliability of the computational results.

Table 2. Binding Energies (kcal/mol) of Target Compounds with SDH

no.	ΔE_{vdw}	ΔE_{ele}	ΔG_{pol}	ΔG_{np}	ΔG_{cal}	ΔG_{exp} [a]
W1	−49.70	−27.89	50.32	−4.25	−31.52	−8.11
W2	−48.85	−26.73	45.27	−4.41	−34.71	−9.08
W4	−48.95	−22.02	44.92	−4.32	−30.38	−7.66
W6	−52.29	−27.21	48.78	−4.55	−35.27	−9.42
W7	−50.99	−24.97	45.43	−4.55	−35.08	−9.19
W8	−51.34	−24.62	44.57	−4.44	−35.83	−9.68
W10	−52.35	−26.08	47.27	−4.56	−35.72	−9.66
W11	−50.33	−19.56	41.35	−4.52	−33.06	−8.86
W12	−53.21	−25.41	47.32	−4.99	−36.28	−10.21
W13	−51.21	−22.34	44.74	−4.50	−33.31	−8.98
W15	−50.90	−21.25	42.43	−4.50	−34.21	−9.03
W16	−48.58	−21.06	41.92	−4.46	−32.19	−8.69
W17	−47.07	−23.64	43.13	−4.34	−31.93	−8.49

[a] $\Delta G_{exp} = -RTLnIC_{50}$.

The binding mode of compound **W12** with SDH is shown in Figure 2A. The compound showed a conserved binding mode compared with commercial SDHI fungicides, forming hydrogen bonds (H-bonds) with B_W173 and D_Y91 and a cation-π interaction with C_R46. The binding mode demonstrates the importance of the silyl moiety for attaining an optimal fit with the entrance to the SDH binding site via the formation of hydrophobic interactions, and therefore for increasing compound fungicidal activity. As shown in Figure 2B, the distal phenyl ring substituted with tripropyl-Si in **W12** reverses the spatial configuration of the inhibitor by 180 degrees, greatly increasing the complementarity at the entrance of the SDH binding site due to the formation of hydrophobic interactions with D_Y91. A similar phenomenon was observed in the other target compounds (Figure 3S, SI). Moreover, the Anal module in Amber9 was used to calculate the VDW energies between the inhibitor and some key residues in the SDH binding site (Figure 4S, SI). The VDW energies between **W1−W17** and D_Y91, C_I43, and C_R46 residues ranged from −5.62 to −7.78 kcal/mol, −4.98 to −8.01 kcal/mol, and −5.04 to −7.96 kcal/mol, respectively, which were far larger than those of flubeneteram (−2.45, −3.49, and −4.12 kcal/mol, respectively). In addition, the ΔE_{vdw} accounts for the greatest contribution to ΔG_{cal} (Table 2). Therefore, the nature of the VDW interactions between the inhibitor and SDH plays an important role in improving compound activity and, by employing the C−Si switch strategy, strengthening these interactions and therefore increasing the inhibition of silyl-flubeneteram analogues.

Fungicidal Activities in a Greenhouse Environment. The fungicidal activities of all of the target compounds were evaluated against some important crop diseases, such as soybean rust (SBR), wheat powdery mildew (WPM), rice blast (RB), cucumber downy mildew (CDM), and soybean gray mold (SGM), in a greenhouse environment. The recently developed SDH commercial fungicides pydiflumetofen, benzovindiflupyr, and isoflucypram were used as the positive controls, and the results are presented in Tables 3, 2S, and 3S (SI), respectively. It is noteworthy that **W1−W17** exhibit particularly strong fungicidal activity against *P. pachyrhizi* Sydow, which causes SBR and is the most significant economic threat to soybean growers all over the world, especially in Brazil. When the crop was treated at a concentration of 100 mg/L, disease control effects against SBR were greater than 90% for most compounds, except **W6−W7, W9, W11−W12,** and **W14**. Moreover, when the dosage was reduced from 100 to 6.25 mg/L, the control effect of most compounds was directly dependent on their concentration. Even at a low dosage of 6.25 mg/L, compounds **W2−W4, W8, W13,** and **W15−W17** still had a protective effect with control of over 90% against SBR. However, the fungicidal activities of these compounds for other diseases, such as WPM, RB, CDM, and SGM, were very low at dosages of 6.25 mg/L. Subsequently, the compound candidates with the most promising fungicidal activities (control effect > 80%) were selected for further experiments at lower dosages ranging from 0.19 to 3.13 mg/L

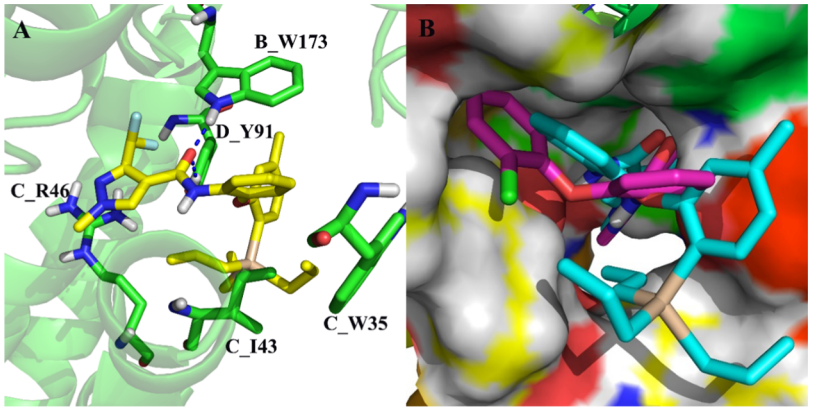

Figure 2. (A) Binding mode of **W12** with SDH. (B) Binding mode overlay of **W12** (cyan sticks) with flubeneteram (magenta sticks).

https://doi.org/10.1021/acs.jafc.0c07322
J. Agric. Food Chem. 2021, 69, 3965−3971

Table 3. Fungicidal Activity of the Target Compounds in Greenhouse

	Soybean rust		
	C (mg/L)/control effect (%)		
no.	100 (mg/L)	25 (mg/L)	6.25 (mg/L)
W1	98	85	35
W2	100	98	98
W3	96	96	90
W4	99	98	98
W5	98	88	85
W6	50	20	0
W7	80	65	30
W8	99	98	85
W9	55	50	40
W10	99	98	80
W11	45	35	20
W12	25	5	0
W13	100	100	92
W14	45	35	30
W15	98	98	95
W16	95	95	90
W17	98	95	90
pydiflumetofen	70	35	10
benzovindiflupyr	99	99	99
isoflucypram	98	85	80

(Table 4). At a concentration of 0.78 mg/L, the control effect against SBR varied widely among different fungicides, including the positive controls, and often showed marked decreases from higher concentrations of the compound; for instance, the control in the commercial fungicide isoflucypram decreased from 80% at 6.25 mg/L to 30% at 0.78 mg/L. In contrast, compounds **W2** and **W8** had a greater protective effect than isoflucypram at 0.78 mg/L with 80% control against SBR, similar to that of the lead compound flubeneteram (78% control) and slightly lower than that of benzovindiflupyr (90% control). We should notice that benzovindiflupyr was the most potent SDHI fungicide against SBR at present. Interestingly, when the concentration was decreased to 0.38 mg/L, **W2** still had a protective effect with control of 80%, considerably higher than that of all of the positive controls (flubeneteram: 20% control, isoflucypram: 20% control, benzovindiflupyr: 50% control). The superiority of **W2** over lead compound flubeneteram can be observed by the fact that while at the very low dosage of 0.19 mg/L, flubeneteram shows no control, and **W2** still maintains control of 30%. Furthermore, the logP values for **W2** (6.45) and flubeneteram (5.19), calculated using tools from the Molinspiration website,[40] are indicative of the greater lipophilicity of **W2** (imparted as a result of the C−Si exchange strategy) and might be an important factor explaining its enhanced fungicidal activity. These results suggest that the incorporation of the trimethyl-silyl group into the flubeneteram scaffold plays a key role in increasing fungicidal activities, especially at very low treated concentrations.

In addition, the EC_{50} value was elucidated for some of the more potent target compounds, as well as the positive controls for comparison. Compound **W2** (EC_{50} = 0.21 mg/L) had the greatest inhibitory effect, impressively even higher than that of the positive controls (flubeneteram: EC_{50} = 0.76 mg/L, benzovindiflupyr: EC_{50} = 0.30 mg/L, isoflucypram: EC_{50} = 1.99 mg/L).

Field Trials. To further study the potential of compound **W2** against SBR, field experiments were performed during the soybean-growing season. Two commercial fungicides with different modes of action (MOA), benzovindiflupyr (targeting SDH), and azoxystrobin (targeting the respiratory chain cytochrome bc_1 complex) were selected as positive controls. As presented in Table 5 and Figure 5S (SI), compound **W2** exhibited good inhibitory activity (72% control) against SBR at 100 mg/L, which was superior to that exhibited by

Table 5. Control Effect of W2 against Soybean Rust in Field Trial

products	control effect (%)
W2 50 (mg/L)	68
W2 100 (mg/L)	72
W2 200 (mg/L)	80
benzovindiflupyr 100 (mg/L)	96
25% azoxystrobin SC 100 (mg/L)	68
CK	80% (disease index)

Table 4. Fungicidal Activity and EC_{50} Value of the Target Compounds in Greenhouse

	Soybean rust						
	C (mg/L)/control effect (%)						
no.	3.13	1.56	0.78	0.38	0.19	EC_{50}(mg/L)	confidence limit 95% (mg/L)
W2	98	95	80	80	30	0.21	0.05−0.33
W3	30	25	20	/[a]	/	/	/
W4	80	65	45	/	/	/	/
W5	40	40	0	/	/	/	/
W8	88	85	80	15	10	0.54	0.31−0.90
W10	80	68	60	/	/	/	/
W13	65	10	10	/	/	/	/
W15	92	85	75	/	/	/	/
W16	70	65	50	/	/	/	/
W17	88	70	65	/	/	/	/
flubeneteram	100	98	78	20	0	0.76	0.69−0.85
benzovindiflupyr	96	95	90	50	40	0.30	0.17−0.43
isoflucypram	40	35	30	20	5	1.99	1.57−2.72

[a]Not tested.

https://doi.org/10.1021/acs.jafc.0c07322
J. Agric. Food Chem. 2021, 69, 3965−3971

azoxystrobin (68% control) but lower than that of benzovindiflupyr (90% control). As we all know, SDH belongs to membrane protein and the transmembrane ability of compound **W2** might be lower than that of benzovindiflupyr, and this affected its fungicidal activity. Therefore, the results indicate that **W2** is the most promising candidate among our synthesized analogues **W1**−**W17** to be a lead compound for the development of novel SDHIs.

In summary, to increase the fungicidal activity, the carbon−silicon switch strategy was used in the design and synthesis of a series of flubeneteram-silyl derivatives. The more potent compounds from this class showed excellent fungicidal activity not only in vitro but also in vivo. Among them, compound **W2** (Figure 1) showed a fungicidal activity against SBR at a very low concentration of 0.19 mg/L, comparable to that of benzovindiflupyr but higher than that of flubeneteram in greenhouse experiments. The results suggest **W2** is a strong candidate for the development of novel silylated fungicides of the pyrazole-carboxamide class against SBR. SAR studies indicate that silyl substitution at C-2 of the distal phenyl ring is essential for increasing the compound's fungicidal activity. Computational results identified the important role of the substituted silyl group for the formation of strong VDW interactions with some key residues in the SDH binding site, suggesting that the flubeneteram-silyl scaffold represents a useful building block from which to develop novel SDHIs.

■ ASSOCIATED CONTENT

Supporting Information

The Supporting Information is available free of charge at https://pubs.acs.org/doi/10.1021/acs.jafc.0c07322.

Enzymatic and fungicidal assays; field trials; X-ray crystal structure of compound W2; correlation between ΔG_{cal} and ΔG_{exp}; binding modes overlay of W1−W17; VDW energies; crystal data of compound W2; antifungal activity of the target compounds in greenhouse; general synthetic procedure; and ^{1}H NMR, ^{13}C NMR, and HRMS spectral data (PDF)

■ AUTHOR INFORMATION

Corresponding Authors

Xiao-Lei Zhu − *Key Laboratory of Pesticide and Chemical Biology of Ministry of Education, International Joint Research Center for Intelligent Biosensor Technology and Health of Ministry of Science and Technology, Central China Normal University, Wuhan 430079, People's Republic of China;* orcid.org/0000-0002-5672-5209; Phone: 86-27-67867800; Email: xlzhu@mail.ccnu.edu.cn; Fax: 86-27-67867141

Guang-Fu Yang − *Key Laboratory of Pesticide and Chemical Biology of Ministry of Education, International Joint Research Center for Intelligent Biosensor Technology and Health of Ministry of Science and Technology, Central China Normal University, Wuhan 430079, People's Republic of China; Collaborative Innovation Center of Chemical Science and Engineering, Tianjin 300071, People's Republic of China;* orcid.org/0000-0003-4384-2593; Email: gfyang@mail.ccnu.edu.cn

Authors

Ge Wei − *Key Laboratory of Pesticide and Chemical Biology of Ministry of Education, International Joint Research Center for Intelligent Biosensor Technology and Health of Ministry of Science and Technology, Central China Normal University, Wuhan 430079, People's Republic of China*

Ming-Wei Huang − *Key Laboratory of Pesticide and Chemical Biology of Ministry of Education, International Joint Research Center for Intelligent Biosensor Technology and Health of Ministry of Science and Technology, Central China Normal University, Wuhan 430079, People's Republic of China*

Wen-Jie Wang − *Key Laboratory of Pesticide and Chemical Biology of Ministry of Education, International Joint Research Center for Intelligent Biosensor Technology and Health of Ministry of Science and Technology, Central China Normal University, Wuhan 430079, People's Republic of China*

Yuan Wu − *Key Laboratory of Pesticide and Chemical Biology of Ministry of Education, International Joint Research Center for Intelligent Biosensor Technology and Health of Ministry of Science and Technology, Central China Normal University, Wuhan 430079, People's Republic of China*

Shu-Fen Mei − *Key Laboratory of Pesticide and Chemical Biology of Ministry of Education, International Joint Research Center for Intelligent Biosensor Technology and Health of Ministry of Science and Technology, Central China Normal University, Wuhan 430079, People's Republic of China*

Li-Ming Zhou − *Key Laboratory of Pesticide and Chemical Biology of Ministry of Education, International Joint Research Center for Intelligent Biosensor Technology and Health of Ministry of Science and Technology, Central China Normal University, Wuhan 430079, People's Republic of China*

Long-Can Mei − *Key Laboratory of Pesticide and Chemical Biology of Ministry of Education, International Joint Research Center for Intelligent Biosensor Technology and Health of Ministry of Science and Technology, Central China Normal University, Wuhan 430079, People's Republic of China*

Complete contact information is available at: https://pubs.acs.org/10.1021/acs.jafc.0c07322

Author Contributions

[§]G.W. and M.-W.H. contributed equally to this work.

Funding

The research was supported in part by the National Key Research and Development Program of China (2018YFD0200100), the National Natural Science Foundation of China (Nos. 21977035, 21837001, and 21772057), and the Key Research and Development Program of Hubei Province (2020BBA052).

Notes

The authors declare no competing financial interest.

■ ACKNOWLEDGMENTS

This paper is dedicated to Professor Youyou Tu, the 2015 Nobel Prize Laureate of Physiology or Medicine, on the occasion of her 90th birthday and the 100th anniversary of chemistry at Nankai University.

■ REFERENCES

(1) Ramesh, R.; Reddy, D. S. Quest for Novel Chemical Entities through Incorporation of Silicon in Drug Scaffolds. *J. Med. Chem.* **2018**, *61*, 3779−3798.

(2) Gately, S.; West, R. Novel therapeutics with enhanced biological activity generated by the strategic introduction of silicon isosteres into known drug scaffolds. *Drug Dev. Res.* **2007**, *68*, 156−163.

(3) Bains, W.; Tacke, R. Silicon chemistry as a novel source of chemical diversity in drug design. *Curr. Opin. Drug Discovery Dev.* **2003**, *6*, 526−543.
(4) Franz, A. K.; Wilson, S. O. Organosilicon Molecules with Medicinal Applications. *J. Med. Chem.* **2013**, *56*, 388−405.
(5) Mills, J. S.; Showell, G. A. Exploitation of silicon medicinal chemistry in drug discovery. *Expert Opin. Invest. Drugs* **2004**, *13*, 1149−1157.
(6) Showell, G. A.; Mills, J. S. Chemistry challenges in lead optimization: silicon isosteres in drug discovery. *Drug Discovery Today* **2003**, *8*, 551−556.
(7) Pooni, P. K.; Showell, G. A. Silicon switches of marketed drugs. *Mini-Rev. Med. Chem.* **2006**, *6*, 1169−1177.
(8) Fujii, S.; Hashimoto, Y. Progress in the medicinal chemistry of silicon: C/Si exchange and beyond. *Future Med. Chem.* **2017**, *9*, 485−505.
(9) Patani, G. A.; Lavoie, E. J. Bioisosterism: A Rational Approach in Drug Design. *Chem. Rev.* **1996**, *96*, 3147−3176.
(10) Lima, L. M.; Barreiro, E. J. Bioisosterism: a useful strategy for molecular modification and drug design. *Curr. Med. Chem.* **2005**, *12*, 23−49.
(11) Meanwell Nicholas, A. Synopsis of Some Recent Tactical Application of Bioisosteres in Drug Design. *J. Med. Chem.* **2011**, *54*, 2529−2591.
(12) Johansson, T.; Weidolf, L.; Popp, F.; Tacke, R.; Jurva, U. In Vitro Metabolism of Haloperidol and Sila-Haloperidol: New Metabolic Pathways Resulting from Carbon/Silicon Exchange. *Drug Metab. Dispos.* **2010**, *38*, 73−83.
(13) Tacke, R.; Popp, F.; Müller, B.; Theis, B.; Burschka, C.; Hamacher, A.; Kassack, M. U.; Schepmann, D.; Wünsch, B.; Jurva, U.; Wellner, E. Sila-Haloperidol, a Silicon Analogue of the Dopamine (D2) Receptor Antagonist Haloperidol: Synthesis, Pharmacological Properties, and Metabolic Fate. *Chemmedchem* **2008**, *3*, 152−164.
(14) Bikzhanova, G. A.; Toulokhonova, I. S.; Gately, S.; West, R. Novel silicon-containing drugs derived from the indomethacin scaffold: Synthesis, characterization and evaluation of biological activity. *Silicon Chem.* **2007**, *3*, 209−217.
(15) Henry, M. J. Mode of action of the fungicide flusilazole in Ustilago maydis. *Pest Manage. Sci.* **1990**, *28*, 35−42.
(16) EFSA. Peer review of the pesticide risk assessment of the active substance silthiofam European Food Safety Authority (EFSA). *EFSA J.* **2016**, *14*, No. e04574.
(17) Koyanagi, T.; Haga, T. Bioisosterism in agrochemicals. *ACS Symp. Ser.* **1995**, *584*, 15−24.
(18) Zhou, C.; Cheng, J.; Beadle, R.; Earley, F. G.; Li, Z.; Maienfisch, P. Design, synthesis and acaricidal activities of Cyflumetofen analogues based on carbon-silicon isosteric replacement. *Bioorg. Med. Chem.* **2020**, *28*, No. 115509.
(19) Xiong, L.; Li, H.; Jiang, L. N.; Ge, J. M.; Yang, W. C.; Zhu, X. L.; Yang, G. F. Structure-Based Discovery of Potential Fungicides as Succinate Ubiquinone Oxidoreductase Inhibitors. *J. Agric. Food Chem.* **2017**, *65*, 1021−1029.
(20) Li, H.; Gao, M. Q.; Chen, Y.; Wang, Y. X.; Zhu, X. L.; Yang, G. F. Discovery of Pyrazine-Carboxamide-Diphenyl-Ethers as Novel Succinate Dehydrogenase Inhibitors via Fragment Recombination. *J. Agric. Food Chem.* **2020**, *68*, 14001−14008.
(21) Chen, T.; Xiong, H.; Yang, J. F.; Zhu, X. L.; Qu, R. Y.; Yang, G. F. Diaryl Ether: A Privileged Scaffold for Drug and Agrochemical Discovery. *J. Agric. Food Chem.* **2020**, *68*, 9839−9877.
(22) Pazenok, S.; Lui, N.; Kosten, M.; Bartels, G. Method for producing 5-fluorine-1-alkyl-3-fluoralkyl-1h-pyrazol-4 carbolic acid chlorides. EP2501682A12012.
(23) Yoshikawa, Y.; Katsuta, H.; Kishi, J.; Yanase, Y. Structure-activity relationship of carboxin-related carboxamides as fungicide. *J. Pestic. Sci.* **2011**, *36*, 347−356.
(24) Nishide, K.; Ohsugi, S.-i.; Miyamoto, T.; Kumar, K.; Node, M. Development of Odorless Thiols and Sulfides and Their Applications to Organic Synthesis. *Monatsh. Chem.* **2004**, *135*, 189−200.
(25) Inaoka, D. K.; Shiba, T.; Sato, D.; Balogun, E. O.; Sasaki, T.; Nagahama, M.; Oda, M.; Matsuoka, S.; Ohmori, J.; Honma, T.; Inoue, M.; Kita, K.; Harada, S. Structural Insights into the Molecular Design of Flutolanil Derivatives Targeted for Fumarate Respiration of Parasite Mitochondria. *Int. J. Mol. Sci.* **2015**, *16*, 15287−15308.
(26) Huey, R.; Morris, G. M.; Olson, A. J.; Goodsell, D. S. A semiempirical free energy force field with charge-based desolvation. *J. Comput. Chem.* **2007**, *28*, 1145−1152.
(27) Morris, G. M.; Goodsell, D. S.; Halliday, R. S.; Huey, R.; Hart, W. E.; Belew, R. K.; Olson, A. J. Automated docking using a Lamarckian genetic algorithm and an empirical binding free energy function. *J. Comput. Chem.* **1998**, *19*, 1639−1662.
(28) Zhu, X. L.; Zhang, M. M.; Liu, J. J.; Ge, J. M.; Yang, G. F. Ametoctradin is a Potent Q(o) Site Inhibitor of the Mitochondria! Respiration Complex III. *J. Agric. Food Chem.* **2015**, *63*, 3377−3386.
(29) Srinivasan, J.; Cheatham, T. E.; Cieplak, P.; Kollman, P. A.; Case, D. A. Continuum Solvent Studies of the Stability of DNA, RNA, and Phosphoramidate−DNA Helices. *J. Am. Chem. Soc.* **1998**, *120*, 9401−9409.
(30) Zhu, X. L.; Xiong, L.; Li, H.; Song, X. Y.; Liu, J. J.; Yang, G. F. Computational and experimental insight into the molecular mechanism of carboxamide inhibitors of succinate-ubquinone oxidoreductase. *Chemmedchem* **2014**, *9*, 1512−21.
(31) Fisher, N.; Bourges, I.; Hill, P.; Brasseur, G.; Meunier, B. Disruption of the interaction between the Rieske iron-sulfur protein and cytochrome b in the yeast bc1 complex owing to a human disease-associated mutation within cytochrome b. *Eur. J. Biochem.* **2004**, *271*, 1292−1298.
(32) Fisher, N.; Brown, A. C.; Sexton, G.; Cook, A.; Windass, J.; Meunier, B. Modeling the Qo site of crop pathogens in Saccharomyces cerevisiae cytochrome b. *Eur. J. Biochem.* **2004**, *271*, 2264−2271.
(33) Guan, A.; Liu, C.; Chen, W.; Yang, F.; Xie, Y.; Zhang, J.; Li, Z.; Wang, M. Design, Synthesis, and Structure−Activity Relationship of New Pyrimidinamine Derivatives Containing an Aryloxy Pyridine Moiety. *J. Agric. Food Chem.* **2017**, *65*, 1272−1280.
(34) Guan, A. Y.; Wang, M. A.; Yang, J. L.; Wang, L. Z.; Xie, Y.; Lan, J.; Liu, C. L. Discovery of a New Fungicide Candidate through Lead Optimization of Pyrimidinamine Derivatives and Its Activity against Cucumber Downy Mildew. *J. Agric. Food Chem.* **2017**, *65*, 10829−10835.
(35) Xiong, L.; Li, H.; Jiang, L. N.; Ge, J. M.; Yang, W. C.; Zhu, X. L.; Yang, G. F. Structure-Based Discovery of Potential Fungicides as Succinate Ubiquinone Oxidoreductase Inhibitors. *J. Agric. Food Chem.* **2017**, *65*, 1021−1029.
(36) Guan, A.; Liu, C.; Huang, G.; Li, H.; Hao, S.; Xu, Y.; Xie, Y.; Li, Z. Synthesis and fungicidal activity of fluorine-containing chlorothalonil derivatives. *J. Fluorine Chem.* **2014**, *160*, 82−87.
(37) Guan, A.; Qin, Y.; Wang, J.; Li, B. Synthesis and insecticidal activity of novel dihalopropene derivatives containing benzoxazole moiety: A structure−activity relationship study. *J. Fluorine Chem.* **2013**, *156*, 120−123.
(38) Smart, B. E. Fluorine substituent effects (on bioactivity). *J. Fluorine Chem.* **2001**, *109*, 3−11.
(39) Maienfisch, P.; Hall, R. G. The Importance of Fluorine in the Life Science Industry. *CHIMIA Int. J. Chem.* **2004**, *58*, 93−99.
(40) Molinspiration Cheminformatics https://www.molinspiration.com/.

https://doi.org/10.1021/acs.jafc.0c07322
J. Agric. Food Chem. 2021, 69, 3965−3971